

Nucleon charge exchange in the $(\pi, \pi N)$ reaction at resonance energies

Y. Ohkubo* and N. T. Porile

Department of Chemistry, Purdue University, West Lafayette, Indiana 47907

(Received 18 November 1981)

The semiclassical trajectory model of Benioff, which treats the nuclear structure of the target by means of the harmonic oscillator model, has been adapted to the $(\pi, \pi N)$ reaction in the (3,3) resonance region. Excitation functions have been calculated for comparison with the experimental results on the following reactions: $^{12}\text{C}(\pi^\pm, \pi^\pm n)$, $^{25}\text{Mg}(\pi^\pm, \pi^\pm p)$, and $^{197}\text{Au}(\pi^\pm, \pi^\pm n)$. The nucleon charge exchange probability P was treated as an adjustable parameter and found to decrease from ~ 0.2 for light elements to ≤ 0.05 for heavy elements. The value of P for ^{12}C is supported by a parameter-free estimate on the basis of a modified free nucleon-nucleon scattering model. The decrease in P with increasing target A is attributed to nuclear size and structure effects. The calculated excitation functions are in good agreement with the experimental results for both light and heavy target nuclei. Experiments that would constitute a more stringent test of various aspects of the model are proposed.

[NUCLEAR REACTIONS $^{12}\text{C}(\pi^\pm, \pi^\pm n)$, $^{25}\text{Mg}(\pi^\pm, \pi^\pm p)$,
 $^{197}\text{Au}(\pi^\pm, \pi^\pm n)$, $T_\pi = 100 - 300$ MeV; calculated excitation functions and
 and nucleon charge exchange probability.]

I. INTRODUCTION

Ever since the first measurement by Reeder and Markowitz,¹ the excitation functions of $(\pi, \pi N)$ ($N = n$ or p) reactions induced in complex nuclei by pions spanning the (3,3) resonance energy have attracted considerable interest. Because the excitation functions mirror the behavior of the free pion-nucleon cross sections, it was expected that σ^-/σ^+ , the ratio of the $(\pi^-, \pi^- n)$ to $(\pi^+, \pi^+ n)$ cross sections on the same target, should display a similar value at the resonance as that of the free π - n cross sections, i.e., three. It thus came as a surprise when Chivers *et al.*² reported a ratio of unity for the single neutron removal reaction on ^{12}C and several other light targets. Although the currently accepted value of σ^-/σ^+ for ^{12}C at the resonance is 1.59 ± 0.07 (Ref. 3), the discrepancy with the free particle ratio persists. Monte Carlo intranuclear cascade (INC) calculations, which modify the free particle ratio by taking into account factors that must play a role in a nuclear target, e.g., Fermi motion, Pauli blocking, final state interactions, two-step mechanisms, etc., thus predict $\sigma^-/\sigma^+ = 2.4$ for ^{12}C at the resonance.^{4,5} Although the experimental and calculated values appear to be ap-

proaching each other the discrepancy is, if anything, more serious because both values are generally believed to be credible.

The most successful explanation of the σ^-/σ^+ ratios for light target elements^{3,6,7} has been given by Sternheim and Silbar (SS).^{8,9} Their model, which developed from an earlier analysis by Hewson,¹⁰ is based on the idea that a nucleon struck by the incident pion can undergo charge exchange (CEX) before leaving the nucleus. The charge exchange probability was estimated by a semiclassical colinear transport calculation and was found to be sufficiently large to lead to a substantial reduction in σ^-/σ^+ from the free-particle value. An impressive fit to the energy dependence of σ^-/σ^+ was obtained with a single normalization at one energy.

The success of the SS calculation was rather puzzling because the ingredients of their model were presumably included in a more complete form in the INC calculation.^{4,5} Sternheim and Silbar¹¹ examined the possible differences between their approach and the cascade model. Although they speculated that offsetting approximations in their model might lead to the resulting difference from the INC predictions, they were unable to arrive at any firm conclusions. More recently, Karol¹² has

reexamined the colinear transport charge exchange model from this point of view. He finds that a questionable averaging procedure in the SS calculation results in an overestimation of the nucleon CEX probability. Karol further reports that a modified version of this calculation predicts σ^-/σ^+ values in accord with the INC calculation^{4,5} and thus, in discrepancy with the experiment.³ An additional problem with the SS model is its inability to predict the σ^-/σ^+ ratios for heavy element targets,⁷ whereas the INC calculations give an adequate fit to the data. It thus appears that a definitive explanation of the magnitudes of the $(\pi^\pm, \pi^\pm N)$ cross sections and their ratios remains to be advanced.

The failure of models that do not take the detailed structure of the target nucleus into account is perhaps not surprising, and has long been known to be the case for the analogous reaction induced by protons. Since single nucleon removal reactions place severe constraints on the energy that can be transferred to the struck nucleus, the reaction site is localized to the nuclear periphery. The cross section then depends on the details of the radial density distribution, and since the latter is a function of the shell model eigenstate of the struck nucleon, the nuclear structure of the target must be taken into account. It was shown by Benioff¹³ that the cross sections of (p, pn) reactions could be reproduced by a colinear transport calculation in which the radial distribution of nucleons in specific shell model states was obtained by means of a harmonic oscillator potential.

The present work consists of an adaptation of the Benioff model¹³ to the $(\pi, \pi N)$ reaction, with particular emphasis placed on the role of nucleon charge exchange. Two major modifications are required in order to make the model applicable to the reaction of interest. First, the 0° scattering angle approximation (colinear transport) assumed for high-energy p - N scattering must be abandoned since it is not valid for π - N scattering at intermediate energies. Second, the present calculation must consider two consecutive interactions, namely, the initial π - N collision and the final state interaction of the struck nucleon. In contrast, Benioff only had to evaluate the cross section for a single p - N interaction. Although the cross section for this sequential process can be evaluated and the probability for nucleon charge exchange thereby determined explicitly, this procedure is not very practical. In our formulation, each collision requires a fivefold integration [see Eq. (4)], so that a calculation of π - N scattering in-

volving a final state interaction would require a tenfold integration. Instead of resorting to this procedure we have chosen to treat the nucleon CEX probability as a parameter whose value is obtained from a fit to the experimental σ^-/σ^+ ratios. The calculation thus yields the excitation functions of $(\pi, \pi N)$ reactions as well as the systematics of the variation of the CEX probability with pion energy and target A .

The calculation is described in Sec. II and the results presented in Sec. III. The reactions chosen for comparison with experiment^{3,7} are $^{12}\text{C}(\pi, \pi n)$, $^{25}\text{Mg}(\pi, \pi p)$, and $^{197}\text{Au}(\pi, \pi n)$. The dependence of the CEX probability on target A is examined and experiments that are more sensitive to this process than those performed to date are proposed. The effect of a possible neutron skin in neutron-rich nuclei on the $(\pi, \pi N)$ reaction is explored and an experimental test of this effect is suggested. The discussion concludes with a modified free nucleon-nucleon analysis of the $^{12}\text{C}(\pi, \pi n)$ reaction that yields an estimate of the CEX probability in a parameter-free way. The agreement between this result and the one based on the modified Benioff treatment lends further weight to the validity of the latter.

II. CALCULATION OF $(\pi, \pi N)$ CROSS SECTIONS

Benioff's¹³ calculation of the (p, pn) cross section uses a classical trajectory approach for the incident and emitted particles (impulse approximation), while the struck nucleon is treated quantum mechanically by use of the shell model with a harmonic oscillator potential. His calculation involves the determination of the probability of an incident proton reaching a particular point in the nucleus, colliding with a nucleon in a specified quantum state, with both nucleons and the produced pions leaving the nucleus without further interaction. The probability is summed over all available nucleons, i.e., those whose removal leaves the residual nucleus in a particle-bound state. In addition to the assumptions made by Benioff, we assume that the effect of the absorption channel on the scattering channel is not significant for $(\pi, \pi N)$ reactions. Furthermore, we neglect final state interactions of the outgoing pion. On the basis of an adaptation of the calculation described below, we find that the probability of such interactions is negligibly small. As indicated above, the zero degree scattering ap-

proximation is replaced by an integration over angle by use of the known π - N differential cross sections.

The basic expressions for calculating the cross sections are as follows:

$$\begin{aligned}\sigma^- &= \sigma_{\text{cl}}(\pi^-, \pi^- n) + P\sigma_{\bar{\text{cl}}}(\pi^-, \pi^- p), \\ \sigma^+ &= \sigma_{\text{cl}}(\pi^+, \pi^+ n + \pi^0 p) + P\sigma_{\bar{\text{cl}}}(\pi^+, \pi^+ p)\end{aligned}\quad (1)$$

for single neutron removal, and

$$\begin{aligned}\sigma^+ &= \sigma_{\text{cl}}(\pi^+, \pi^+ p) + P\sigma_{\bar{\text{cl}}}(\pi^+, \pi^+ n), \\ \sigma^- &= \sigma_{\text{cl}}(\pi^-, \pi^- p + \pi^0 n) + P\sigma_{\bar{\text{cl}}}(\pi^-, \pi^- n)\end{aligned}\quad (2)$$

for single proton removal. The designation cl for "clean" refers to a single collision process, i.e., the incident pion goes through the nucleus without interaction until it strikes a nucleon whose removal leaves the residual nucleus in a bound state; the outgoing pion and struck nucleon escape without further interaction. The designation $\bar{\text{cl}}$ for "unclean" refers to a process which differs from the above

only in the fact that the outgoing nucleon interacts with the nucleus in some way (final state interaction). The quantity P is the fraction of $\sigma_{\bar{\text{cl}}}$ involving nucleon charge exchange. The above designations are similar in meaning to those commonly used in (p, pN) reactions.¹⁴

The quantity σ_{cl} is given by

$$\sigma_{\text{cl}} = \sum_{\substack{\text{allowed} \\ nlj \text{ values}}} N_{nlj} \sigma_{nl}, \quad (3)$$

where N_{nlj} stands for the number of neutrons or protons in the shell specified by the conventional quantum numbers n , l , and j . The sum is over the allowed n , l , and j values for which the removal of a nucleon leaves the residual nucleus particle-stable. If $\sigma_{\pi N}$ is the total π - N scattering cross section, $\sigma_{nl}/\sigma_{\pi N}$ can be understood as the fractional availability of a nucleon in the n, l shell for single collision processes. Since we employed the harmonic oscillator model, the j subscript has been dropped from σ . The expression for σ_{nl} , whose derivation is given elsewhere,¹⁵ is

$$\begin{aligned}\sigma_{nl} &= \frac{2^{(l+1)}}{(\pi)^{1/2}(2l+c)!!} \\ &\times \int_{\theta_{\min}}^{\pi/2} \frac{d\sigma_{\pi N}}{d\Omega}(\theta) \sin\theta d\theta \int_0^{2\pi} d\phi \int_0^\infty u du \int_{-\infty}^\infty dv B_n^2(u^2+v^2)^l \\ &\times \exp \left\{ -u^2 - v^2 - \frac{\beta^2}{\pi^{3/2}} \int_{-\infty}^v \sum_{\nu} \sigma_{\pi_{\text{in}}}^{\text{tot}}(\nu) \rho_{\text{in}}^{\pi}(\nu) d\nu \right. \\ &\quad \left. - \frac{\beta^2}{\pi^{3/2}} \int_v^\infty \sum_{\nu} [\sigma_{\pi_{\text{out}}}^{\text{tot}}(\nu) \rho_{\text{out}}^{\pi}(\nu) \right. \\ &\quad \left. + \sigma_{N_{\text{out}}}^{\text{tot}}(\nu) \rho_{\text{out}}^N(\nu)] d\nu \right\} \\ &+ \frac{2^{(l+1)}}{\pi^{1/2}(2l+c)!!} \int_{\pi/2}^{\pi} \frac{d\sigma_{\pi N}}{d\Omega}(\theta) \sin\theta d\theta \\ &\times \int_0^{2\pi} d\phi \int_0^\infty u du \int_{-\infty}^\infty dv B_n^2(u^2+v^2)^l \\ &\times \exp \left\{ -u^2 - v^2 - \frac{\beta^2}{\pi^{3/2}} \int_{-\infty}^v \sum_{\nu} [\sigma_{\pi_{\text{in}}}^{\text{tot}}(\nu) \rho_{\text{in}}^{\pi}(\nu) \right. \\ &\quad \left. + \sigma_{\pi_{\text{out}}}^{\text{tot}}(\nu) \rho_{\text{out}}^{\pi}(\nu)] d\nu \right. \\ &\quad \left. - \frac{\beta^2}{\pi^{3/2}} \int_v^\infty \sum_{\nu} \sigma_{N_{\text{out}}}^{\text{tot}}(\nu) \rho_{\text{out}}^N(\nu) d\nu \right\}. \quad (4)\end{aligned}$$

The first term in Eq. (4) is concerned with forward pion scattering ($\theta \leq \pi/2$) and the second term with backward scattering ($\pi/2 \leq \theta \leq \pi$). The use of a minimum scattering angle θ_{\min} as the lower limit of the integration over θ assures that the outgoing nucleon has enough energy to escape from the nucleus. The values of θ_{\min} were obtained from kinematics by use of experimental separation energies of the struck nucleons.¹⁶ In essence, the expression involves an integration over the differential cross section for π - N scattering multiplied by exponential attenuation factors. The definitions of the important symbols are summarized in Table I. Benioff's article¹³ may be consulted for more complete details. Figure 1 shows the cylindrical coordinate system employed.

The harmonic oscillator spring constant β in the exponents of Eq. (4) can be written as

$$\beta^2 = 0.8472/A^{1/3}r_0^2, \quad (5)$$

where r_0 is the half central density radius constant.¹³ The variables u , v , and w are related to the coordinates r , z , and y in Fig. 1 through β :

$$u = \beta r, \quad v = \beta z, \quad \text{and} \quad w = \beta y.$$

The ν -type nucleon (neutron or proton) density expression $\rho(\nu)$ in the exponential factors in Eq. (4) is given by

$$\rho(\nu) = \sum_{nl} \nu_{nl} \frac{2^l B_n^2}{(2l+c)!!} x^l \exp(-x), \quad (6)$$

with

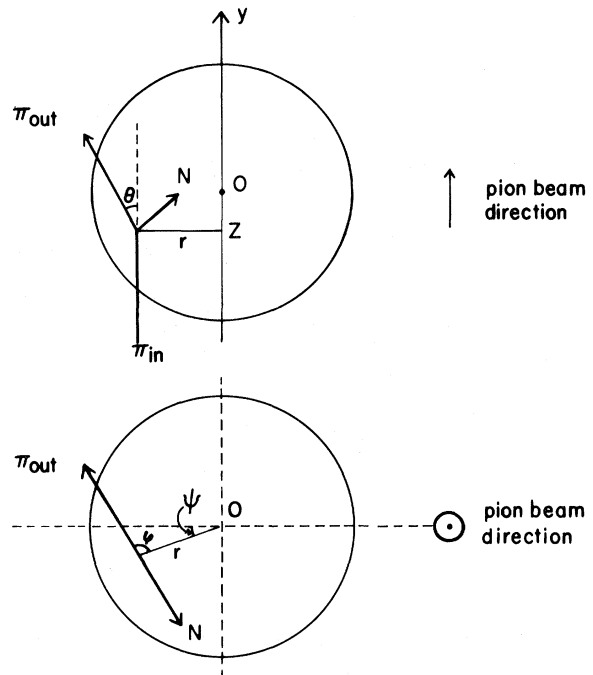


FIG. 1. Cylindrical coordinate system employed. The upper figure is with respect to the scattering angle θ (polar angle). The collision takes place at coordinates r , ψ , and z . The lower figure is with respect to the azimuth ϕ .

$$x = u^2 + v^2$$

for the incident pion,

$$x = u^2 + w^2 + (w - v)^2 \tan^2 \theta - 2u(w - v) \tan \theta \cos \phi$$

TABLE I. Definitions of symbols employed.

N_{nlj}	The number of nucleons in the quantum states specified by the quantum numbers n , l , and j (principal, orbital angular momentum, and total angular momentum).
θ, ϕ	Pion scattering angles (polar and azimuthal).
θ_{\min}	Minimum scattering angle at which the outgoing nucleon has just enough kinetic energy to escape from the residual nucleus.
$\frac{d\sigma_{\pi N}}{d\Omega}$	Free π - N differential cross section in the laboratory system.
ν	ν -type nucleon (proton or neutron).
$\sigma_{\pi_{\text{in}}}^{\text{tot}}(\nu)$	Total cross section for the scattering between the incident pion and the ν -type nucleon in the residual nucleus.
$\sigma_{\mu_{\text{out}}}^{\text{tot}}(\nu)$	Total cross section for scattering between the outgoing μ -type particle (pion or struck nucleon, $\mu = \pi$ or N) and the ν -type nucleon.
$\rho_{\text{in}}^{\pi}(\nu)$	ν -type nucleon density seen by the incident pion.
$\rho_{\text{out}}^{\mu}(\nu)$	ν -type nucleon density seen by the outgoing μ -type particle ($\mu = \pi$ or N).
β	Harmonic oscillator spring constant.
M, μ	Nucleon mass (938.3 MeV/ c^2) and pion mass (139.6 MeV/ c^2).

for the outgoing pion, and

$$x = u^2 + w^2 + (w - v)^2 \tan^2[\sin^{-1}(F \sin\theta)] \\ + 2u(w - v) \tan[\sin^{-1}(F \sin\theta)] \cos\phi$$

for the outgoing nucleon. The quantity F is related to the law of momentum conservation:

$$F = [T_\pi^{\text{out}}(T_\pi^{\text{out}} + 2\mu) / T_N^{\text{out}}(T_N^{\text{out}} + 2M)]^{1/2}. \quad (7)$$

The expressions for $\sigma_{\bar{c}l}$ are obtained by replacing the exponential factor for the outgoing nucleon in Eq. (4), i.e.,

$$\exp \left[-\frac{\beta^2}{\pi^{3/2}} \int_v^\infty \sum_N \sigma_{N_{\text{out}}}^{\text{tot}}(v) \rho_{\text{out}}^N(v) dw \right],$$

with

$$1 - \exp \left[-\frac{\beta^2}{\pi^{3/2}} \int_v^\infty \sum_N \sigma_{N_{\text{out}}}^{\text{tot}}(v) \rho_{\text{out}}^N(v) dw \right]. \quad (8)$$

The free π - N differential and total cross sections were calculated from the phase shifts of Rowe *et al.*¹⁷ $\sigma_{\pi^0 N}^{\text{tot}}$ was calculated from isospin considerations:

$$\sigma_{\pi^0 N}^{\text{tot}} = \frac{1}{2} (\sigma_{\pi^+ p}^{\text{tot}} + \sigma_{\pi^- p}^{\text{tot}}). \quad (9)$$

For the outgoing nucleon, the free nucleon-nucleon scattering cross section expressions were taken from Chen *et al.*¹⁸

As indicated in Eq. (5), the calculation requires input values of r_0 for the various targets of interest. For ^{12}C , r_0 was taken directly from the tabulated values based on electron scattering experiments^{19,20} since for this nucleus the harmonic oscillator model was used to obtain r_0 . This procedure could not be used for the heavier targets as the tabulated r_0 are based on the use of the Fermi density distribution. In these instances r_0 was obtained by fitting a harmonic oscillator distribution to the Fermi distribution in the region of the nuclear surface. The procedure is illustrated for ^{197}Au in Fig. 2. The Fermi distribution, which yields $r_0 = 1.11$ fm, can be fitted in the nuclear surface with a harmonic oscillator distribution with $r_0 = 0.95$ fm. Note that the two curves differ in the central region of the nucleus. This difference has a negligible effect on the calculated $(\pi, \pi N)$ cross section in view of the fact that the reaction site is localized to the nuclear surface. Also shown in Fig. 2 is the harmonic oscillator distribution for the same r_0 value as the Fermi distribution, i.e., 1.11 fm. This choice is clearly unacceptable as it greatly overestimates the surface density.

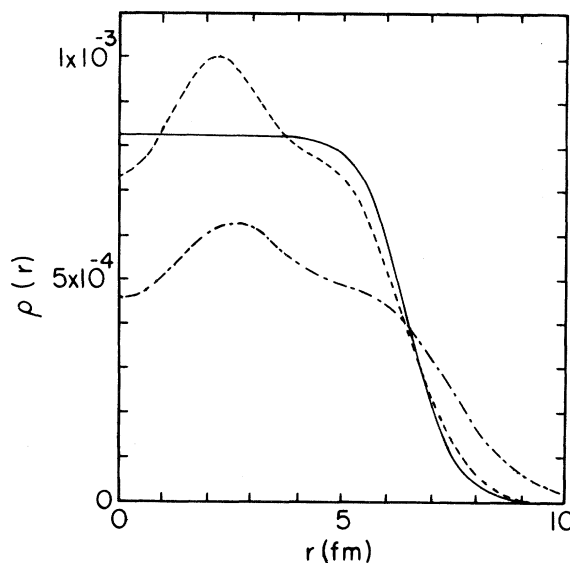


FIG. 2. Proton densities in ^{197}Au . $\rho(r)$ is normalized so that integration over the r coordinate gives unity. Solid curve: Fermi distribution $\rho(r) \sim [1 + e^{(r-r_0)^{1/3}/c}]^{-1}$ with $r_0 = 1.11$ fm, $c = 0.529$ fm, and $A = 197$ (Refs. 19 and 20); dashed curve, adjusted harmonic oscillator distribution with $r_0 = 0.95$ fm; dotted-dashed curve, harmonic oscillator distribution with $r_0 = 1.11$ fm.

Table II lists the available shells for the $(\pi, \pi N)$ reactions of interest,^{13,21,22} the nucleon separation energies, the r_0 values employed, and for comparison, the corresponding Fermi distribution r_0 . Note that only certain proton or neutron shells are listed as being available for the unclean process in spite of the fact that these nucleons remain in the nucleus. In view of the small probability that following the CEX interaction the struck nucleon repopulates the level from which it was ejected by the pion, the residual nucleus would be left in an unbound state unless the nucleon in question was originally in an available level.

The calculation was performed by numerical integration of Eq. (4) for $\sigma_{\bar{c}l}$ and of Eq. (4) with Eq. (8) for $\sigma_{\bar{c}l}$. The grid sizes for the angle integrations (θ and ϕ) were 30° . The cutoff values and the number of grids for the u , v , and w integrations were chosen so that the difference in the numerical integration due to different grid sizes and cutoff values was less than 1% for ^{12}C and ^{25}Mg and than 2% for ^{197}Au . The values of the charge exchange probability P in Eqs. (1) and (2) were obtained from a fit to the experimental cross section ratios.

TABLE II. Available shells, separation energies, and r_0 values employed.

Target nucleus	Available shells (Refs. 13, 21, and 22)	Separation energy (Ref. 16) (MeV)	r_0 (fm)	Fermi r_0 (Refs. 19 and 20) (fm)
^{12}C	$1p_{3/2}(4)^a n$ for σ_{cl}	18.7	1.04	
	$1p_{3/2}(4)p$ for $\sigma_{\bar{\text{cl}}}$	16.0		
^{25}Mg	$1d_{5/2}(4)p$ for σ_{cl}	12.1	1.06	1.06
	$1d_{5/2}(5)n$ for $\sigma_{\bar{\text{cl}}}$	7.3		
^{197}Au	$3p_{3/2}(4), 1i_{13/2}(14), 1h_{9/2}(10)$	8.1 ^b	0.95	1.11
	$2f_{7/2}(8)n$ for σ_{cl}			
	$1g_{7/2}(8), 1h_{11/2}(12), 2d_{3/2,5/2}(9)p$ for $\sigma_{\bar{\text{cl}}}$	5.8 ^b		
^{18}O	$1d_{5/2}(2)n^c$	8.05	1.07	
	$1p_{3/2,1/2}(6)p$	15.94		

^aThe number in parenthesis is the number of nucleons.

^bThe listed separation energy is that for the least bound nucleon.

^cFor ^{17}O formation, n for σ_{cl} , p for $\sigma_{\bar{\text{cl}}}$; for ^{17}N formation, n for $\sigma_{\bar{\text{cl}}}$, p for σ_{cl} .

III. RESULTS AND DISCUSSION

A. Comparison with experimental results

The results of the calculation are compared with the corresponding experimental results for the ^{12}C , ^{25}Mg , and ^{197}Au targets in Figs. 3–5, respectively. In each of these figures, panel (a) displays the calculated charge exchange probability P , panels (b) and (c) the calculated and experimental excitation functions for π^- or π^+ as well as the values of σ_{cl} only, and panel (d) the experimental values of σ^-/σ^+ [σ^+/σ^- for $^{25}\text{Mg}(\pi, \pi p)$] along with the clean cross section ratios and the free particle ratios. The uncertainties in the values of P and in those of σ^\pm are based exclusively on those in the corresponding experimental cross section ratios.

The calculated excitation functions are generally in very good agreement with experiment, particularly in the vicinity of the resonance. In this respect, the results are more satisfactory than those from either the SS or the INC calculations since agreement is obtained for both light and heavy target elements. The calculation does appear to underestimate the cross sections for ^{12}C at the higher energies, and those for ^{197}Au at both high and low energies, while the agreement for ^{25}Mg is excellent throughout. The discrepancy for ^{197}Au , particularly at the low energies, undoubtedly reflects the contribution of inelastic scattering followed by evaporation to the experimental cross section. As pointed out by

Kaufman *et al.*,⁷ the INC calculation predicts a sizable contribution from this mechanism to the $(\pi, \pi n)$ reaction on heavy elements at energies well below the resonance and to a lesser extent, at 300 MeV as well. From another point of view, Sternheim and Silbar²³ have considered the effect of such factors as pion production and Fermi motion on the $^{12}\text{C}(\pi, \pi n)$ reaction at higher energies. While these effects appear to be significant above 400 MeV, they are negligible at 300 MeV and so cannot constitute the source of the observed discrepancy for this target.

Figures 3–5 indicate that the charge exchange contribution to the $(\pi^-, \pi^- n)$ or $(\pi^+, \pi^+ p)$ reactions is very small, the clean knockout process accounting for the bulk of the calculated cross section. On the other hand, charge exchange is seen to contribute to a significant extent to the $(\pi^+, \pi^+ n)$ and $(\pi^-, \pi^- p)$ reactions, particularly for light targets. These results reflect the fact that the $\pi^- - n$ (or $\pi^+ - p$) scattering amplitude is much larger than the $\pi^- - p$ (or $\pi^+ - n$) amplitude. Since the CEX contribution to the $(\pi^+, \pi^+ n)$ reaction results from $\pi^+ - p$ scattering, the effect is much more dramatic than in the case of the corresponding $(\pi^-, \pi^- n)$ reaction.

B. Mass dependence of the charge exchange probability

Figures 3–5 indicate that charge exchange is of importance for light elements, occurring in about

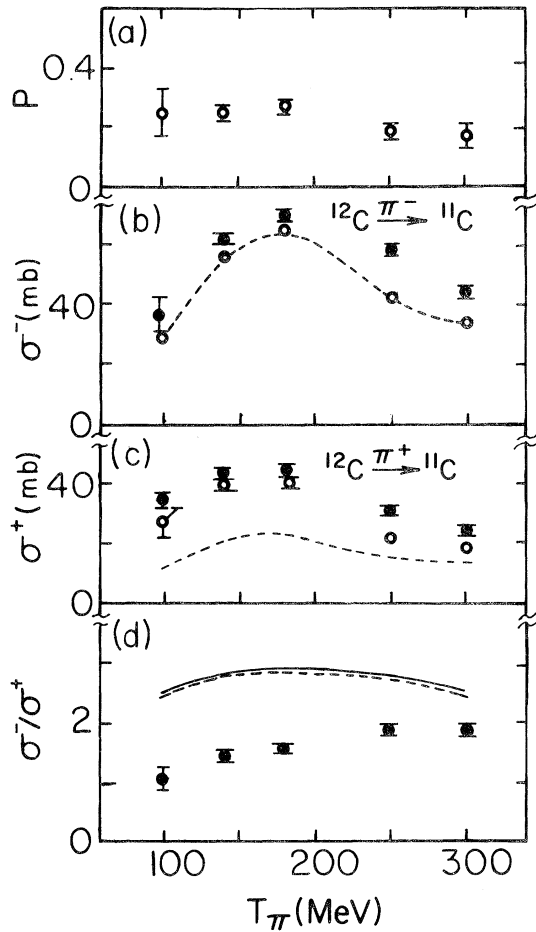


FIG. 3. Cross sections for formation of ^{11}C by π^\pm incident on ^{12}C . Solid points: expt. (Ref. 3); open points: this work with the nucleon charge exchange assumption; dashed curve: this work with $P=0$; solid curve: free particle ratio.

20% of the final state interactions. On the other hand, CEX is relatively unimportant for heavy elements, where it occurs in $\leq 5\%$ of the final state interactions. We believe that two distinct effects are responsible for the low P values for heavy elements: multiple collisions of the outgoing nucleon, and the formation of residual nuclei unstable with respect to further particle emission as a result of CEX.

For neutron removal reactions, the first effect can be understood in terms of the ratio R of σ_{cl}^+ per available proton to σ_{cl}^- per available neutron. (For proton removal R is defined as the ratio of σ_{cl}^- per available neutron to σ_{cl}^+ per available proton.) The difference between these two cross sections per available nucleon primarily reflects the scattering

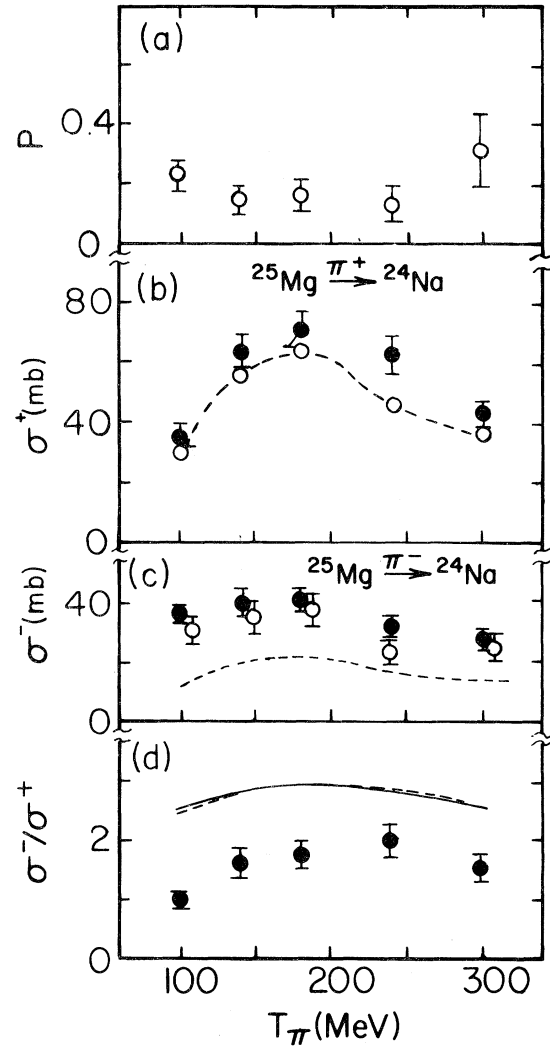


FIG. 4. Cross sections for formation of ^{24}Na by π^\pm incident on ^{25}Mg . Experimental data from Ref. 7. See Fig. 3 for significance of symbols and curves.

probability of the outgoing nucleon. For a self-conjugate target, a value of unity for R means that the outgoing nucleon has a 50% chance of being scattered while a large value of R corresponds to a scattering probability close to unity. These values are slightly different for a target with $N \neq Z$ because of differences in the attenuation of π^+ and π^- , but this effect is small. Table III lists the values of R obtained at 180 MeV for the three targets of interest. Note that R is approximately twice as large for a heavy element as for a light one indicating that final state interactions are of greater importance for the former. It is also possible to inter-

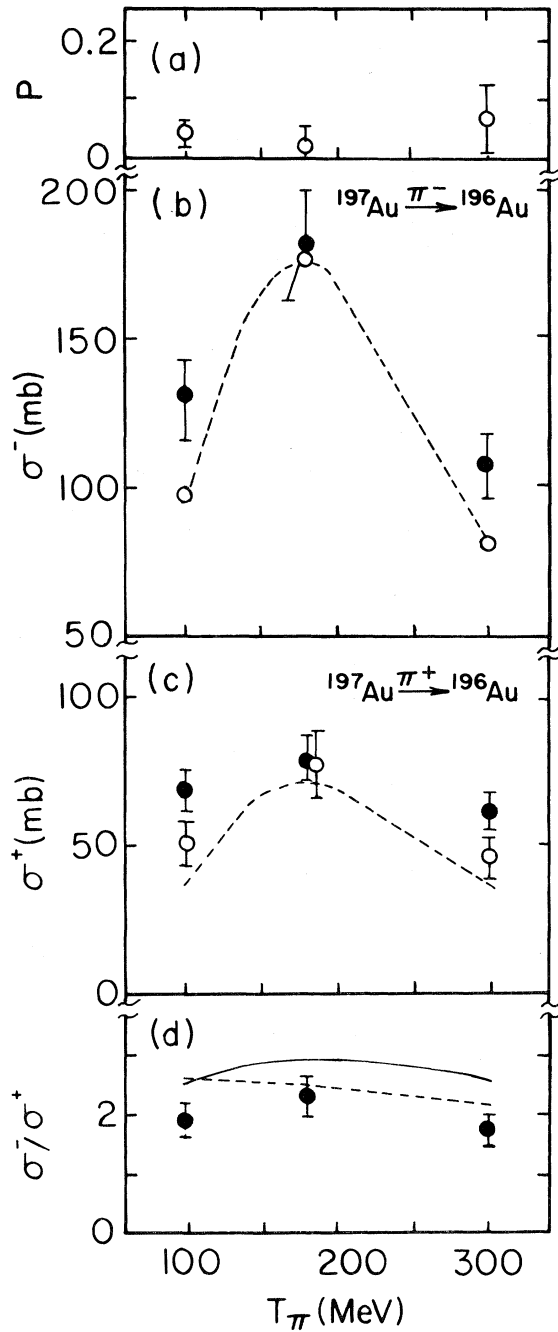


FIG. 5. Cross sections for formation of ^{196}Au by π^\pm incident on ^{197}Au . Experimental data from Ref. 7. See Fig. 3 for significance of symbols and curves.

pret R as a measure of the number of collisions undergone by the outgoing nucleon. If the scattering probability is large, the outgoing nucleon is thus more likely to scatter more than once than if the

TABLE III. Multiple scattering ratio R and the nuclear size effect.

	$^{12}\text{C} \rightarrow ^{11}\text{C}$	$^{25}\text{Mg} \rightarrow ^{24}\text{Na}$	$^{197}\text{Au} \rightarrow ^{196}\text{Au}$
R	1.1	1.2	2.2

probability is small. From this point of view the values of R indicate that an outgoing nucleon is likely to undergo about twice as many collisions in a large nucleus as in a small one. These additional collisions can have a variety of outcomes. The nucleon can thus undergo a second charge exchange, eject a second nucleon, transfer enough excitation energy to the residual nucleus to render it unstable with respect to particle emission, etc. All these outcomes have one feature in common, namely, they reduce the value of P for heavy elements. In view of the dependence of the multiple scattering probability on volume, we shall refer to this effect as the nuclear size effect.

The second effect results from the fact that for a light target the protons and neutrons participating in CEX generally tend to occupy the same shell model states, with the number of available neutrons being comparable to the number of unavailable neutrons. On the other hand, for heavy elements the available neutrons and protons occupy different shells, with the number of unavailable neutrons being much larger than the number of available ones. Figures 6 and 7 show how these factors affect the CEX probability. Figure 6 shows the radial dependence of (a) the ratio of the $1p_{3/2}$ neutron density (available neutrons) in ^{12}C to the $1s_{1/2}$ neutron density (unavailable) and (b) the $1p_{3/2}$ proton density (available) in the same nucleus. At the maximum of the $1p_{3/2}$ proton density, the ratio in the upper figure is about 1.5. Roughly speaking, the outgoing proton, which used to be in the $1p_{3/2}$ orbital, will in the unclean process strike a $1p_{3/2}$ neutron with a somewhat greater probability than a $1s_{1/2}$ neutron. Since the emission of the latter leaves the nucleus unbound with respect to further particle emission, the probability of CEX leading to an unbound residue is ~ 0.4 . This picture is, of course, very crude and should not be taken seriously in an absolute sense since the actual probability of striking a $1s_{1/2}$ nucleon must be small (see Sec. F). However, we believe that it is of value in a comparison with a similar analysis for ^{197}Au .

Figure 7 shows (a) the ratio of the available neu-

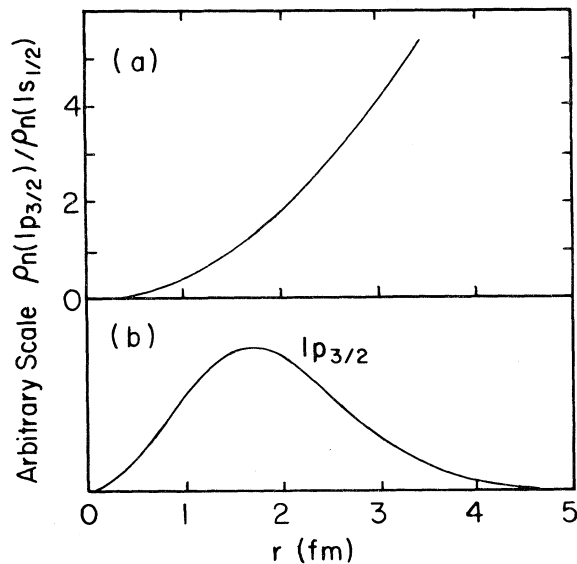


FIG. 6. Nucleon distribution in ^{12}C . The upper figure shows the ratio of the $1p_{3/2}$ neutron density to the $1s_{1/2}$ neutron density. The lower figure gives the $1p_{3/2}$ proton distribution.

tron density ($1h_{9/2}$, $1i_{13/2}$, $2f_{7/2}$, and $3p_{3/2}$) to the unavailable neutron density in ^{197}Au , and (b) the available proton density distribution ($1g_{7/2}$, $1h_{11/2}$, and $2d_{5/2,3/2}$). At the maximum of the available proton density, the ratio in Fig. 7(a) is about 0.25. This result means that if nucleon charge exchange

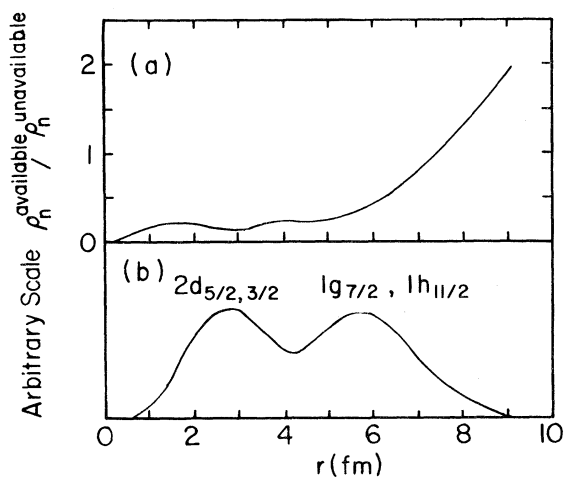


FIG. 7. Nucleon distribution in ^{197}Au . The upper figure shows the ratio of the available neutron density to the unavailable neutron density. The lower figure gives the available proton distribution.

takes place, the residual nucleus has a probability of about 0.8 to be particle unstable. Note that this probability is about twice as large as it is in ^{12}C and thus leads to smaller values of P for heavy elements. We refer to this phenomenon as the nuclear shell effect and conclude that for heavy target elements the magnitude of the contribution of CEX to the $(\pi, \pi N)$ reaction is reduced owing to both the nuclear size and nuclear shell effects.

C. Comparison with other estimates of the CEX probability

The values of P displayed in Figs. 3–5 may be compared with previous estimates of this quantity. For ^{12}C , values of the CEX probability have been obtained by SS⁸ and by Karol.¹² The only previous result available for ^{197}Au is one obtained by scaling⁹ the ^{12}C result of SS to this target. The various values of P are compared in Figs. 8 and 9. It must be noted that this comparison is only approximate since the various authors define P in somewhat different ways.

Figure 8 shows that the present values of P for ^{12}C are in good agreement with those of SS. We are

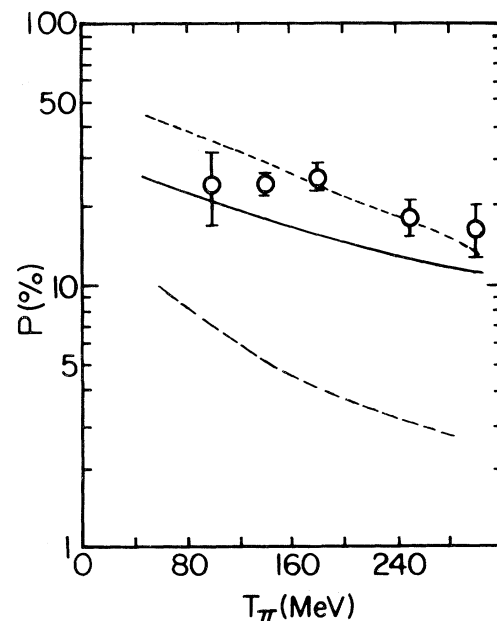


FIG. 8. Nucleon charge exchange probability in ^{12}C . Open circles: Benioff-type calculation, this work; short dashed curve: Sternheim-Silbar calculation (Ref. 8); long dashed curve: Karol's calculation (Ref. 12); solid line: modified free nucleon-nucleon calculation, this work.

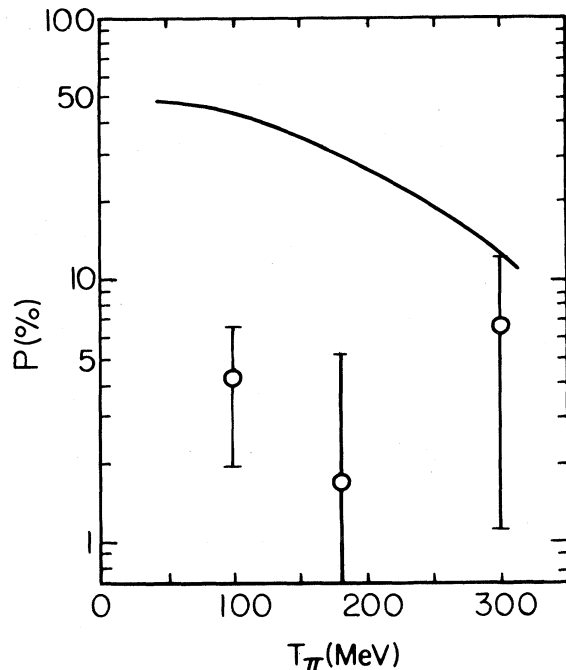


FIG. 9. Nucleon charge exchange probability in ^{197}Au . Open circles: this work; solid curve: Sternheim-Silbar calculation (Refs. 8 and 9).

thus led to the same conclusion as these workers, namely that charge exchange of the outgoing nucleon is important for light nuclei. A closer look at the results does indicate that the present values of P appear to exhibit a smaller energy dependence than the previous values.⁸ We believe that this difference reflects some of the approximations in the SS treatment. For instance, these workers assumed an approximate relation between the outgoing nucleon energy T_N and the incident pion energy T_π , i.e., $T_N = (\frac{1}{3})T_\pi$. In contrast, on the basis of a kinematical calculation based on the π - N differential cross sections we find that T_N does not bear such a constant relation to T_π . Instead, we find that T_N varies from $(1/3.2) T_\pi$ for 100 MeV pions to $(1/4.6) T_\pi$ for 300 MeV pions. As a result, the CEX cross section varies less steeply with pion energy than assumed by SS and our resulting values of P are less energy dependent.

The values of P_{ex} derived by Karol¹² are seen to be much smaller than the present results. His numerical values depend on the assumed values of several parameters, e.g., the Pauli blocking factor, and can be increased substantially by a choice of different and perhaps more reasonable values. We

defer a more detailed discussion of this point to a subsequent section, where a modified version of a free-particle type calculation of P is presented for ^{12}C .

Figure 9 shows a comparison of the present values of P for ^{197}Au with those based on the SS scaling procedure.^{8,9} In contrast to the agreement obtained for ^{12}C , the two sets of values now differ by an order of magnitude. We have already mentioned that nuclear size and structure effects result in a reduction in the CEX probability for heavy elements. These effects are not included in the scaling procedure used by these workers.⁹ In addition, the assumption that π^+ and π^- are equally attenuated from the reaction channel of interest, which is implicit in their model, does not appear to be completely valid for heavy elements as a result of differences in the neutron and proton density in the nuclear surface. This effect is considered in more detail in a subsequent section.

D. Sensitivity of the cross section ratio to the charge exchange probability

The single nucleon removal reactions studied to date do not constitute a very sensitive test of the importance of the CEX process. As shown in Table II, the number of neutrons available for the clean fraction of the $(\pi, \pi n)$ cross section [protons for $(\pi, \pi p)$] is comparable to the number of protons [neutrons for $(\pi, \pi p)$] available for the unclean process. Since the magnitude of the unclean contribution is reduced by the relatively low value of P , the effect of CEX on the values of σ^-/σ^+ or σ^+/σ^- is rather small.

These considerations suggest that a target nucleus having a large number of available protons and a small number of available neutrons would constitute a more sensitive probe of the importance of CEX in the $(\pi, \pi n)$ reaction. Conversely, a target with a large number of available neutrons and a small number of available protons would serve a similar role for the $(\pi, \pi p)$ reaction. A good target from this point of view is ^{18}O . Table II indicates that this nuclide has six available protons and only two available neutrons. Consequently, σ^-/σ^+ should be unusually low if CEX is of importance while σ^+/σ^- should be somewhat larger than similar ratios obtained for target nuclei in the same mass with comparable number of available protons and neutrons. Figure 10 shows our calculated excitation functions and cross section ratios for the

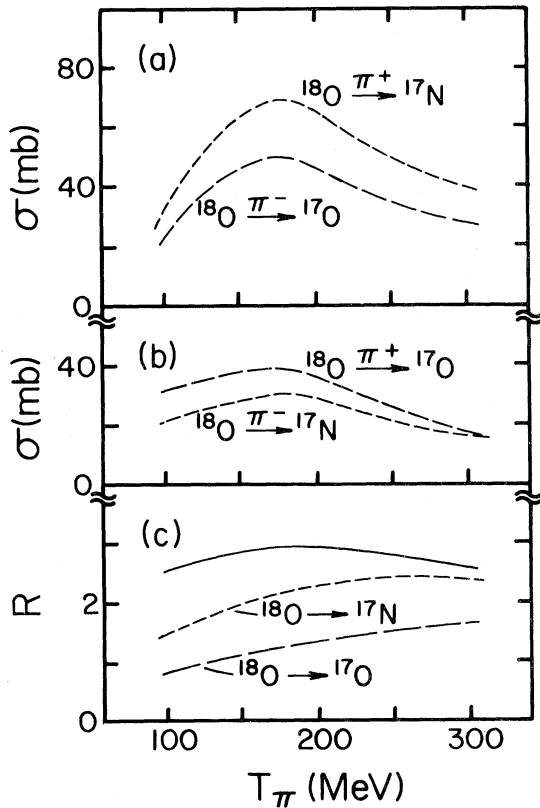


FIG. 10. Calculated excitation functions for the $^{18}\text{O}(\pi^\pm, \pi^\pm n)$ and $^{18}\text{O}(\pi^\pm, \pi^\pm p)$ reactions. The bottom panel shows the cross section ratio, $R = \sigma^-/\sigma^+$ for the $(\pi, \pi n)$ reaction (long dashes) and $R = \sigma^+/\sigma^-$ for the $(\pi, \pi p)$ reaction (short dashes), as well as the free particle ratio (solid curve).

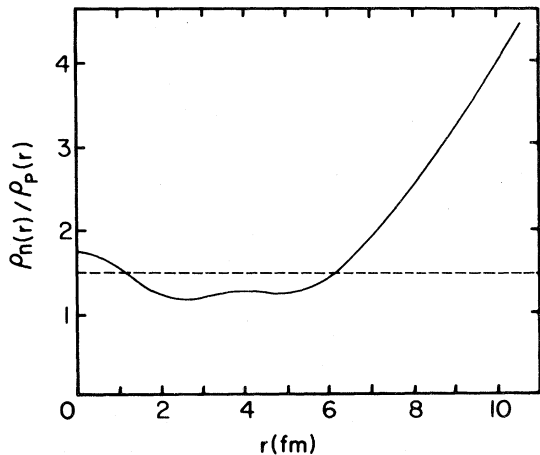


FIG. 11. Radial dependence of ratio of neutron to proton density in ^{197}Au according to harmonic oscillator model. The dashed line is the ratio N/Z .

$^{18}\text{O}(\pi, \pi n)$ and $^{18}\text{O}(\pi, \pi p)$ reactions. The results are based on $P \sim 0.2$, the exact values being obtained by interpolation between the ^{12}C and ^{25}Mg CEX probabilities. Note that the σ^-/σ^+ ratio at the resonance is only ~ 1 while the σ^+/σ^- ratio is ~ 2 . For a target with comparable number of available neutrons and protons, the two ratios should, of course, be practically equal. Note, too, that the cross sections of the $^{18}\text{O}(\pi^-, \pi^- n)$ reaction are rather low compared to those of the $^{12}\text{C}(\pi^-, \pi^- n)$ reaction, for instance. The $^{18}\text{O}(\pi, \pi n)$ cross section could be determined by in-beam γ -ray spectrometry while the $(\pi, \pi p)$ cross section could be measured by observation of the delayed neutrons emitted by ^{17}N . Another interesting target from this point of view is ^{96}Ru , which has a much larger number of available protons than neutrons. However, since the CEX probability may be much smaller in this mass region, the effect may not be as striking.

E. The $(\pi, \pi N)$ reaction as a probe of the neutron density distribution

Since the $(\pi, \pi N)$ reaction occurs as a result of π - N scattering in the nuclear surface, it may be possible to use this reaction to probe the composition of the surface region. While it appears that the neutron density distribution extends to larger radii than the proton distribution for neutron-rich nuclei such as ^{197}Au , the evidence is not definitive.²⁴ The harmonic oscillator model predicts such a difference, as illustrated for ^{197}Au in Fig. 11. If this effect is real, the implications for the $(\pi, \pi N)$ reaction are significant.

As one manifestation of this effect, we focus on the comparison of the clean cross section ratios with the free particle ratios displayed in Figs. 3–5. For light nuclei the two ratios are virtually identical indicating that π^+ and π^- are attenuated to the same extent. On the other hand, for ^{197}Au the clean cross section ratio is significantly lower than the free particle ratio except at the lowest energy, where agreement is obtained. In view of the larger π^- - n scattering amplitude, the π^- flux is attenuated to a larger extent in passing through the neutron skin than the π^+ flux, resulting in a lower value of $\sigma_{cl}^-/\sigma_{cl}^+$. At low energies the small π - N scattering amplitudes lead to a sufficiently long mean free path of the incident and outgoing pions that the difference in the radial extension of neutron and proton shells is of minor consequence. As a result,

the clean cross section ratio reverts to the free particle value. The fact that the calculated ratio of clean cross sections for ^{197}Au agrees with the experimental ratio at the resonance is another manifestation of the fact that the CEX probability is very small.

The $(\pi, \pi p)$ reaction on neutron-rich nuclei constitutes a more interesting probe of the extent of a neutron skin in these nuclei. If such a skin exists, the incident pion must penetrate further into the nucleus before striking a proton. Because of the strong π^-n amplitude, an incident and outgoing π^- will be more strongly attenuated in passing through this neutron rich region than a π^+ . As a result, the $\sigma_{\text{cl}}^+/\sigma_{\text{cl}}^-$ ratio should be larger than the free particle value. Since the CEX probability for heavy elements appears to be very small, this effect should persist for the experimental σ^+/σ^- ratio. In view of the fact that all σ^+/σ^- (or σ^-/σ^+) ratios measured to date are smaller than the free particle ratio, the observation of such an unusual ratio would indicate the action of an as yet unobserved factor. Figure 12 shows our estimate of the cross sections and σ^+/σ^- ratios for the $^{197}\text{Au}(\pi, \pi p)$ reaction, assuming no charge exchange. The reaction could be studied by in-beam γ -ray spectrometry. A similar result should be obtained for the $(\pi, \pi p)$ reaction on neighboring Pt isotopes, e.g., ^{195}Pt , ^{196}Pt , or ^{198}Pt , which can be studied by conventional activation techniques.

F. Evaluation of the CEX probability for ^{12}C by a modified free particle-particle model

Karol¹² has obtained a simple expression for the probability of CEX in ^{12}C by appropriately modifying the semiclassical colinear transport model of Steinheim and Silbar.⁸ In this section we obtain a result for P using an approach that, while in essence similar to that of Karol, is more consistent with our somewhat different definition of P .

Recalling that P is defined in Eq. (1) as the fraction of the unclean cross section involving CEX and leading to a particle-stable residual nucleus, we can express P for ^{12}C as

$$P = \frac{\sigma_{\text{CEX}} \rho'_n}{\sigma_{pp} \rho_p + \sigma_{pn} \rho_n}, \quad (10)$$

where σ_{pp} and σ_{pn} are the free p - p and p - n scattering cross sections, and σ_{CEX} is the charge exchange cross section. The precise definition of the nucleon densities (or numbers) ρ'_n , ρ_n , and ρ_p is most impor-

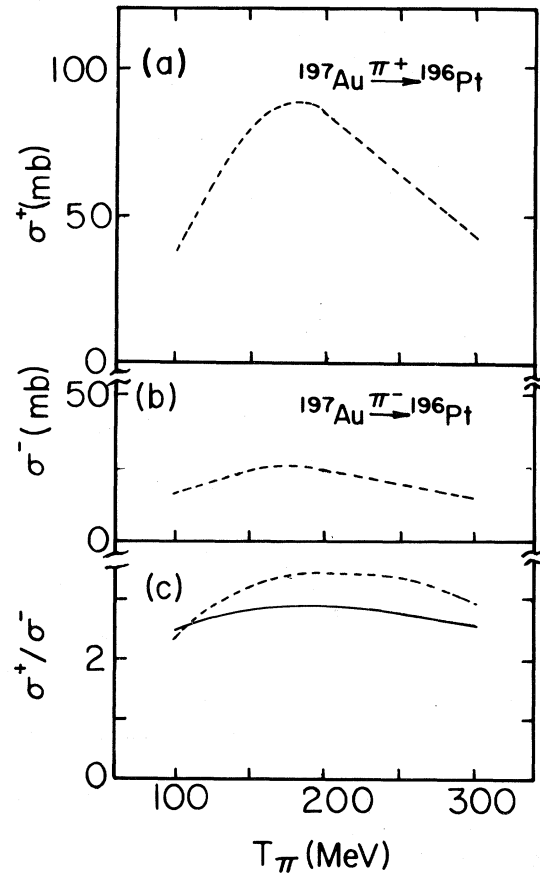


FIG. 12. Calculated cross sections for the $^{197}\text{Au}(\pi^\pm, \pi^\pm p)$ reaction. Dashed curves: calculated excitation functions and σ^+/σ^- ratio for $P=0$; solid curve: free particle ratio.

tant for a realistic evaluation of P since these quantities contain the crucial nuclear structure information that is missing in the free-particle scattering approach. The quantity ρ'_n in the numerator is the number of neutrons available for charge exchange, i.e., the four $1p_{3/2}$ neutrons. The quantities ρ_p and ρ_n are the effective proton or neutron densities, i.e., the number of protons and neutrons that the $1p_{3/2}$ proton struck by the pion in the initial interaction is likely to encounter. We set $\rho_p=3$ and $\rho_n=4$, corresponding to the fact that the struck proton is only likely to interact with the $1p_{3/2}$ nucleons, and not with the $1s_{1/2}$ nucleons. The interaction with the $1s_{1/2}$ nucleons is inhibited by Pauli blocking and by the localization of the $1s_{1/2}$ nucleons to the nuclear core. This assumption is confirmed by our calculation of the attenuation factors, which shows that σ_{cl}^- is essentially independent of whether the $1s_{1/2}$ nu-

cleons are included in the density expression or not. Our calculation differs in this respect from that of Karol, who included the $1s_{1/2}$ nucleons in ρ_n and ρ_p .

We employ the following expressions for σ_{CEX} , σ_{pn} , and σ_{pp} :

$$\sigma_{\text{CEX}} \simeq 5.4 \times 10^4 T_N^{-1.9} \text{ mb}, \quad (11)$$

$$\sigma_{pn} \simeq 1.8 \times 10^4 T_N^{-1.2} \text{ mb}, \quad (12)$$

and

$$\sigma_{pp} \simeq 1/3 \sigma_{pn}, \quad (13)$$

where T_N is in MeV. Equations (12) and (13) are approximations to the more complex expressions for σ_{pn} and σ_{pp} given elsewhere.¹⁸ The expression for σ_{CEX} is based on that of Karol¹² with the following two modifications: First, we neglect Pauli blocking in σ_{CEX} ($\beta=1$, whereas Karol used $\beta=0.45$). This appears to be appropriate for a $1p_{3/2} \rightarrow 1p_{3/2}$ CEX transition since the state that is populated is the analog state. Further, if in the spirit of the free particle model we treat the residual nucleus as a spectator to the CEX interaction, there is no population of the states above the $1p_{3/2}$ level due to Fermi broadening, and thus no Pauli blocking either. Second, we have used the actual separation energy of the $1p_{3/2}$ proton in ^{11}C , i.e., 8.7 MeV in evaluating σ_{CEX} instead of the mean nucleon separation energy, i.e., 11 MeV.

The quantity T_N in Eqs. (11) and (12) is the mean kinetic energy of the outgoing nucleon. As mentioned earlier, we evaluated T_N from the π - N differential cross sections and elementary kinematics. We find that T_N ranges from $(1/3.2) T_\pi$ for 100 MeV pions to $(1/4.6) T_\pi$ at 300 MeV, which yields a somewhat different result for σ_{CEX} than that obtained by SS or Karol, who approximated T_N as $\frac{1}{3} T_\pi$ over the entire energy range.

The resulting values of P are shown in Fig. 8. Note that the agreement with the Benioff type calculation is quite good. Since the values of P obtained in the latter are based on a fit to the experimental cross section ratios while the values of present interest involve no adjustable parameters, the agreement lends support to our formulation of the $(\pi, \pi N)$ problem. The results are in qualitative agreement with the SS calculation and thus support the notion that nucleon CEX is important for light target elements. On the other hand, our values of P are substantially larger than those of Karol, the difference reflecting the combined effect of the above mentioned factors. Because of the simplifica-

tions introduced in this modified free nucleon-nucleon scattering calculation, it is not profitable to extend this approach to target nuclei significantly heavier than ^{12}C .

IV. CONCLUSIONS

The excitation functions of $(\pi, \pi N)$ reactions in the vicinity of the (3,3) resonance have been calculated by an adaptation of Benioff's model of (p, pN) reactions, in which the incident and emitted particles are treated by a classical trajectory formalism while the target nucleus is treated quantum mechanically by use of the harmonic oscillator shell model. The nucleon charge exchange probability P is obtained from a fit to the experimental cross section ratios σ^-/σ^+ ($N=n$) or σ^+/σ^- ($N=p$). A modified free nucleon-nucleon scattering model, which may have some validity for a nucleus with as simple a shell structure as ^{12}C , yields parameter-free values of P which are in agreement with those obtained in our more rigorous but parameter dependent calculation.

The calculated excitation functions for the $^{12}\text{C}(\pi, \pi n)$, $^{25}\text{Mg}(\pi, \pi p)$, and $^{197}\text{Au}(\pi, \pi n)$ reactions are in good agreement with the corresponding experimental results. In this respect, our model is superior to the colinear transport model,⁸ which agrees with the results for light elements but not with those for heavy elements, and to the INC model,^{4,5} which exhibits just the opposite behavior. The incorporation of the structure of the target nucleus into the calculation appears to be necessary in order to obtain agreement over a broad range of target mass and composition. Nucleon charge exchange is found to account for $\sim 20\%$ of the final state interactions in light elements but for only 5% or less of those in heavy elements. We attribute this trend to effects associated with the size and structure of the target nucleus.

The experiments performed to date do not test our model in a critical way. We suggest that experiments on targets with widely different numbers of available neutrons and protons could constitute a more sensitive probe of the importance of nucleon charge exchange. The study of the $(\pi, \pi N)$ reactions of ^{18}O and ^{96}Ru appears to be promising in this respect. The effect of a possible neutron skin in neutron-rich nuclei on $(\pi, \pi N)$ reactions is considered. We show that the study of $(\pi, \pi p)$ reactions on heavy elements is likely to yield results that bear on this problem.

ACKNOWLEDGMENTS

We wish to acknowledge valuable discussions with Dr. L. C. Liu and Dr. P. J. Karol. This work

was made possible by the financial support of the U. S. Department of Energy.

-
- *Present address: Los Alamos National Laboratory, Los Alamos, New Mexico.
- ¹P. L. Reeder and S. S. Markowitz, *Phys. Rev.* **133**, B639 (1964).
- ²D. T. Chivers, E. M. Rimmer, B. W. Allardyce, R. C. Witcomb, J. J. Domingo, and N. W. Tanner, *Nucl. Phys.* **A126**, 129 (1969).
- ³B. J. Dropesky, G. W. Butler, C. J. Orth, R. A. Williams, M. A. Yates-Williams, G. Friedlander, and S. B. Kaufman, *Phys. Rev. C* **20**, 1844 (1979).
- ⁴G. D. Harp, K. Chen, G. Friedlander, Z. Fraenkel, and J. M. Miller, *Phys. Rev. C* **8**, 581 (1973).
- ⁵J. N. Ginocchio, *Phys. Rev. C* **17**, 195 (1978).
- ⁶N. P. Jacob and S. S. Markowitz, *Phys. Rev. C* **13**, 754 (1976).
- ⁷S. B. Kaufman, E. P. Steinberg, and G. W. Butler, *Phys. Rev. C* **20**, 262 (1979).
- ⁸M. M. Sternheim and R. R. Silbar, *Phys. Rev. Lett.* **34**, 824 (1975).
- ⁹R. R. Silbar, J. N. Ginocchio, and M. M. Sternheim, *Phys. Rev. C* **15**, 371 (1977).
- ¹⁰P. W. Hewson, *Nucl. Phys.* **A133**, 659 (1969).
- ¹¹R. R. Silbar, J. N. Ginocchio, and M. M. Sternheim, *Phys. Rev. C* **18**, 2785 (1978).
- ¹²P. J. Karol, *Phys. Rev. C* **23**, 415 (1981).
- ¹³P. A. Benioff, *Phys. Rev.* **119**, 324 (1960).
- ¹⁴J. R. Grover and A. A. Caretto, *Annu. Rev. Nucl. Sci.* **14**, 51 (1964).
- ¹⁵Y. Ohkubo, Ph.D. thesis, Purdue University, 1981.
- ¹⁶A. H. Wapstra and N. B. Gove, *Nucl. Data Tables* **9**, 7 (1971).
- ¹⁷G. Rowe, M. Salomon, and R. H. Landau, *Phys. Rev. C* **18**, 584 (1978).
- ¹⁸K. Chen, Z. Fraenkel, G. Friedlander, J. R. Grover, J. M. Miller, and Y. Shimamoto, *Phys. Rev.* **166**, 949 (1968).
- ¹⁹H. R. Collard, L. R. B. Elton, and R. Hofstadter, *Nuclear Radii* (Springer, Berlin, 1967).
- ²⁰R. C. Barrett and D. F. Jackson, *Nuclear Sizes and Structure* (Clarendon, Oxford, 1977).
- ²¹A. A. Ross, H. Mark, and R. D. Lawson, *Phys. Rev.* **102**, 1613 (1956).
- ²²*Table of Isotopes*, 7th ed., edited by C. M. Lederer and V. S. Shirley (Wiley, New York, 1978).
- ²³M. M. Sternheim and R. R. Silbar, *Phys. Rev.* **24**, 574 (1981).
- ²⁴J. A. Nolen and J. P. Schiffer, *Annu. Rev. Nucl. Sci.* **19**, 471 (1969).